Low Frequency Noise of Few Layer MoS_2

Undergraduate Honor Research Distinction Thesis

Presented in Partial Fulfillment of the Requirements for the Degree of Bachelor of Science with Honor Research Distinction at The Ohio State University

By

Junao Cheng

Department of Electrical and Computer Engineering

The Ohio State University

2017

Dissertation Committee:

Professor Wu Lu, Advisor

Professor Patrick Roblin

Abstract

The study of 2D semiconductor materials has been proposed as one of the most promising candidates to resolve the problem of upcoming limit of CMOS fabrication technology in downscaling. We can further shrink the device channel length and gate thickness to atomic scales considering the thin layer properties of 2D semiconductors. The semiconducting material molybdenum disulfide (MoS_2) has attracted more attention for its possible application of into field-effect transistors (FETs) with its proper energy bandgap. This study therefore investigates the low frequency noise characteristics of the two-terminal few layer 6nm thick MoS_2 device grown by Chemical Vapor Deposition (CVD). We focus on the transport mechanisms of the few layer MoS_2 channel rather than the influence of metal contacts. Studies of the device noise transport characteristics at temperatures ranging from 10K to 296K were conducted regarding different carrier transport mechanisms so as to reveal the relation between these two important device concepts of interest. As it has been revealed before, the carrier transport study suggests that the device is dominated by thermally activated band transport at T>180K, Efros-Schklovskii hopping when 50K<T<180K, and resonant tunneling when T<50K. The low frequency noise result of such device is dominated by mobility fluctuation mechanisms when T>180K, corresponding to the band transport mechanism. Such result could be attributed to the material crystal quality as the mobility increases with increasing temperature, suggesting the dominance of impurity scattering mechanism under all ranges of temperatures measured. Also, the variable range hopping noise signatures are

also observed when 75K<T<180K, which indicated the consistence of low frequency noise study and carrier transport phenomena. When T<50K, ubiquitous phenomenon of non-Lorentzian power spectrum density was observed potentially related to resonant tunneling mechanisms. The study of low frequency noise would be meaningful for further applications of such low dimensional semiconductor materials system considering the high surface to volume ratio. The clarification of various carrier and noise transport mechanisms would be therefore informative for further investigation and development of such materials.

Acknowledgments

I would like to thank Prof. Wu Lu for his sincere advices and help during my study of this topic with him in the past few years. It is Prof. Lu who inspired me on the research of such advanced topic of solid state electronics. He pushed me to take up more responsibilities on mastering various kinds of lab skills and theoretical knowledges.

In addition, I want to thank Hao Yang and Hao Xue for their valuable suggestions and help gave to me when I was conducting this topic of research. Hao Xue helped me on the measurement of low frequency noise spectrum when T<77K using liquid helium as cryogenic resource. Hao Yang helped to set up the computer and instrument interface for performing measurements and extracting data. Therefore, I was able to extract and analyze my experiment results with such a great amount of assistance given by Hao Yang. Also, it was Hao Xue who inspired me on the research of summarizing different noise fluctuation mechanisms leading to one of the most important part of research in this project.

I would like to thank Scott Poehler for his patient training on my lab skills. Scott helped me with initial design of large area open environment chemical vapor deposition of MoS_2 film, and low frequency noise measurement device testing system setup. I would like to thank all other group members, Paul Bertani and Vishank Telestra, who gave me great advices during all group meeting discussions.

Vita

July 2012.....Zhabei No.8 Jr. High

Aug 2012 to Jun 2014.....Shanghai University

Major: Materials Physics

Aug 2014 to May 2017 .....The Ohio State University

B.S. Electrical and Computer Engineering (Honor Program)

B.S. Applied Physics

Fields of Study Major Field: Electrical and Computer Engineering

Table of Contents

List of Figures

Chapter 1: Introduction

1.1 General Introduction of 2D Semiconductive MoS_2 Materials

The electronic device development was limited for further progress in regards of the semiconductor device scaling and performance. Stated by the Moore's Law, the integration of transistors is doubled in approximately every two years. The traditional 3D silicon based electronic device design would reach the limit of integrated circuits as we need to accommodate increasing number of transistors on the limited area of the chip. Potential solutions to this challenge includes the investigation and application of new electronic materials, or apply another possible device design.

The 2D semiconductor family of materials has been suggested to further application in solving such problems by the researchers [1] for its promising performance and thin layer structure in scaling down. The main focus was classified into application [2] of Graphene as an electrical conductor, Hexagonal Boron Nitride (h-BN) as an electrical insulator, and Transition Metal Dichalcogenides (TMDC) as semiconductors. Regardless of MoS_2 or Graphene, they are fairly stable within the 2D layer and connected by Van der Waals [2] forces between layers. The semiconductive material MoS_2, as a typical member of TMDC, has attracted more attention for its possible application in sensors, digital and optical electronics [3,4,5] with its proper energy bandgap. It has a bandgap E_g = 1.2~1.8 eV dependent on the layer thickness [6] while Eg=0 for Graphene without special structure treatment [7]. Few layered MoS_2 materials attracted the attention of research for

its potential of industrial large-scale growth and high speed transport properties. Currently, researchers had demonstrated top-gated MoS_2 devices using HfO_2 as gate dielectric material, back-gated MoS_2 devices on Si/SiO_2 substrates [8] for digital electronics application. Heterojunction devices of WSe_2 and MoS_2 [9], Graphene and MoS_2 [10] suggested its bright future on various field of applications of hetero-tunnel diodes, and flexible electronics. These devices built on 2D MoS_2 are either mechanically exfoliated [11], or grown by chemical vapor deposition [12] (CVD), pulsed laser deposition [13], physical sputtering using RF magnetron system [14] etc.

1.2 Introduction to the Importance of Low Frequency Noise Study

The noise in the circuits refers to the spontaneous fluctuations of the system when measuring or amplifying small input signals [15]. There are two general categories of noise of system: random noise and systematic noise. The first one is generally to be analyzed with multiple statistical and physical theories of the signals. The second one is usually idiosyncratic to the measurement conditions as background noises while could be avoided with proper experiment design setup. Modelling and simulation on the noise characteristics of the circuit is important in defining the physical limits of the signal sensitivity to be applied to the system. The accuracy of measurements and strength of applied signals is defined therefore to ensure the proper operation of the integrated circuit, because the noise cannot be reduced with the increase of measurement time.

Researchers have focused on various noise sources considering their characteristics and applications. For example, the Johnson noise [15] in an electronic component, typically a resistor, could be used to measure the Boltzmann constant with temperature dependent measurement of signal fluctuations; the shot noise [15] in a pin photodiode could be used to measure the electrical unit charge. The low frequency noise, as the main subject of research in this study, is one of the most important component of high frequency phase noise [16]. The study of such topic would be informative for the device characteristics over a wide range of frequencies. Also, the specific properties of the low frequency noise spectrum could be used to analyze some important properties of devices [17]. Analysis of the interfacial trap density of gate and channel, activation energy of trap states could be achieved from the carrier number fluctuation model of low frequency noise transport [17]. One could reduce the system noise through the improvement of device mobility from the estimation of mobility fluctuation model. The general classification of such mechanisms could be summarized in Equation 1, 2. As proposed by Hooge's Empirical Relationship [17], the Normalized Power Spectrum Density could be modeled as shown in Equation below, S_I refers to power spectrum density which is defined as the RMS value of noise signal over a unit range of frequency as shown in Equation 3 below. Further discussion of low frequency noise and carrier transport would be elaborated in Chapter 3 of this article.

$$\frac{\delta I^2}{I^2} = \frac{\delta \mu^2}{\mu^2} + \frac{\delta n^2}{n^2} = Normalized\ Power\ Spectrum\ Density \quad (1)$$

$$\frac{S_I}{I^2} = \frac{\alpha_H}{N} f^{-\beta} = Normalized\ Power\ Spectrum\ Density \quad (2)$$

$$S_I = {< \Delta V^2 >}/{\Delta f} \quad (3)$$

Chapter 2: CVD MoS_2 Materials Growth

2.1 CVD process in close environment furnace

The large area MoS_2 few layered material in this study was grown by chemical vapor deposition (CVD) method on 0001-oriented sapphire substrate through collaborations with Prof. Siddharth Rajan and Yiying Wu's research groups at OSU. In this process, bulk MoS_2 powders were used as sulfur vapor source precursor so that the sulfur would be supplied over a long period of time for the growth of the few layered materials. In this process the tube was evacuated first to create vacuum condition of material growth. The Mo source was first deposited on the sapphire wafer through e-beam evaporation creating uniform and large-area film coverage on the surface. Therefore, the few layer film was achieved by the evaporation of few layer Mo metal on the sapphire surface. As shown in Figure 1 [12], the wafer and MoS_2 powder were placed in separate boats to facilitate the uniform sulfur concentration over growth.

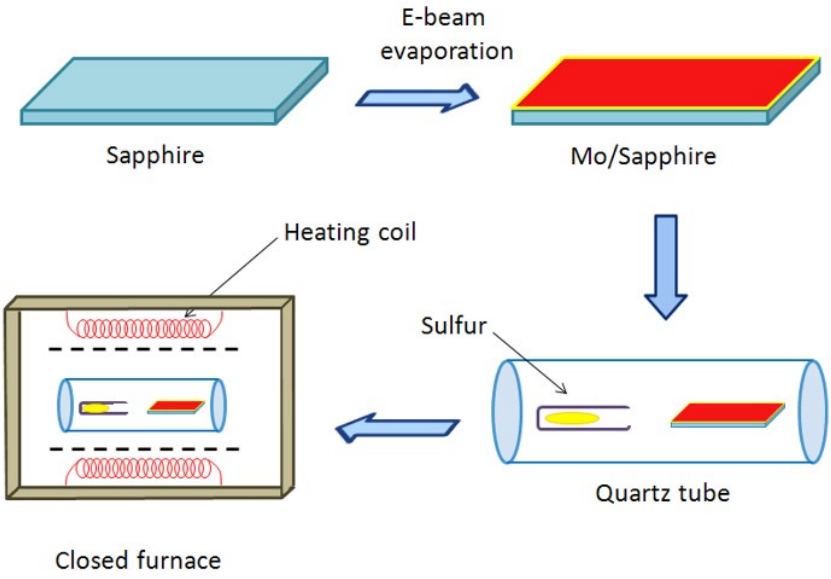

Figure 1: Illustration of large area MoS_2 growth in closed environment [12].

In result, high quality 6 nm thick few layer MoS_2 films are grown confirmed by cross-sectional Transmission electron microscopy (TEM), Raman Spectroscopy, and Atomic Force Micrograph (AFM) as shown in Figure 2a to 2c below [12].

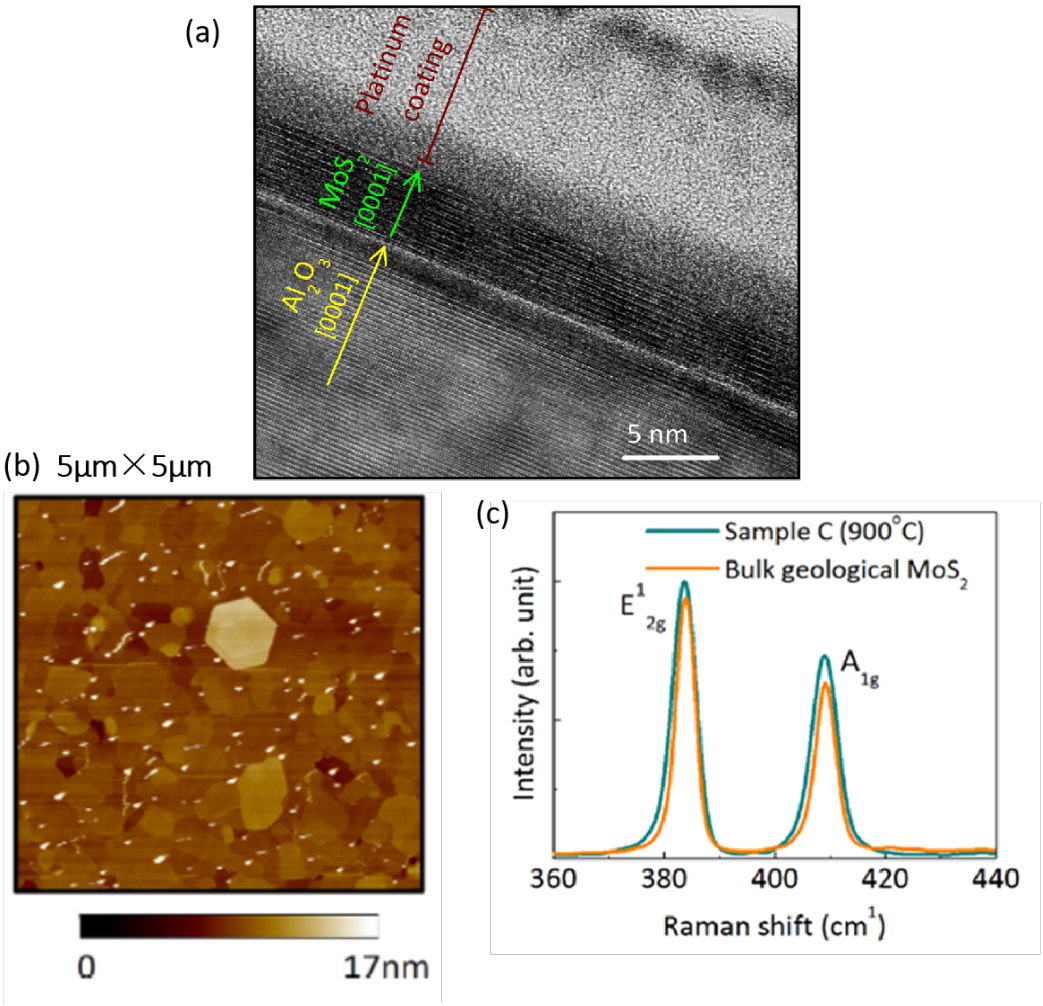

Figure 2 [12]: Few Layer MoS_2 material properties as grown by close environment CVD (a) TEM image showing the 6nm thick channel. Also, the inter layer single crystal structure is confirmed. (b) Raman Spectra showing consistence of CVD grown film and bulk MoS_2 material with two characteristic peak position at $E^1_{2g} = 382$ cm^{-1} and $A_{1g} = 407$ cm^{-1}. (c) Atomic force micrograph on a 5μm×5μm square area implying large area film coverage and hexagonal crystal morphology.

2.2 CVD process in inert gas flowing furnace

Due to potential industrial prospect of large scale and high efficiency growth of MoS_2 materials, we proceed to the design the process of open atmosphere condition growth of material growth using e-beam deposited Mo on (0001) oriented sapphire substrate. In this design, Ar gas was used as inert gas source to reduce the influence of oxidation from the atmosphere. However, the tube scale and Ar gas flow rate limited the success growth in this process. Therefore, we applied Ar gas purging over the furnace tube for 20 min before the process begin for eliminating environmental conditions. And we applied Ar gas purging for another 20 min after the process to reduce sulfur vapors in the tube for safety. In our initial design, uniform furnace temperature coverage was applied over the tube without Ar gas flowing at 1100 ºC with 3 hr growth time. However, the resulting film grown is oxidized resulting in MoO_3 materials spread over the furnace tube and material surface. This gave insight on how precise the temperature and gas environment should be controlled over the furnace.

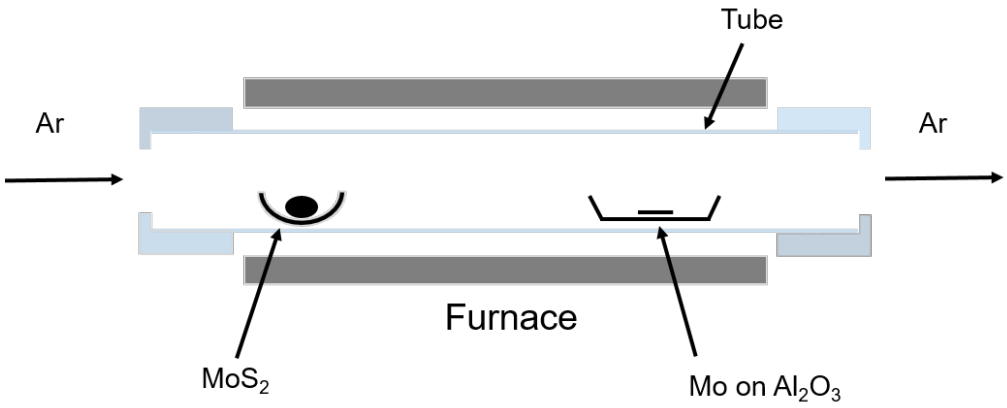

Figure 3: Illustration of large area MoS_2 growth in open atmosphere environment.

After multiple trails and runs, we considered adding Sulfur powder into the furnace to increase the sulfur vapor concentration. Therefore, the Mo film on the wafer surface would have more chances of being reacted into MoS_2 film rather than oxidized. The amount of powder was increased to 5g of MoS_2 powder and 5g of sulfur powder, sustaining a longer period of growth, which is 5 hr considering the dis-association rate of MoS_2 powder into sulfur vapors. Also, we kept Ar gas purging at a higher rate for the entire film growth process to eliminated the interference of oxidation. increased the amount of powder sustaining a longer period of growth, which is 5 hr considering the dis-association rate of MoS_2 powder into sulfur vapors.

In result, we achieved small area materials grown on the surface of the Al_2O_3 as confirmed by Raman Spectroscopy. However, the characteristic Raman shifts only occur at a few laser spot positions on the film grown as shown in Figure 4. The ideal shown here is sample as shown by the close environment furnace as discussed in Chapter 2.1, and sample 144 here is achieved through applied side covers in guiding sulfur vapor to the sample surface with 4 hrs of CVD process at 900ºC.

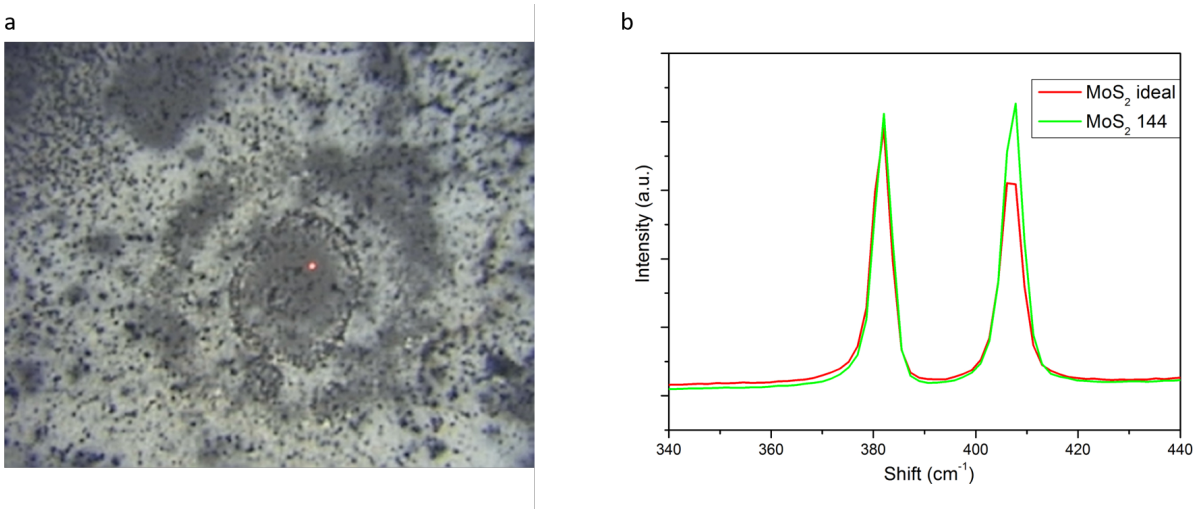

Figure 4: Few Layer MoS2 material properties as grown by open environment CVD (a) Raman Spectra of the optimized sample comparing with ideal case (b) Optical Image of Laser Spot Applied in Raman Spectroscopy.

2.3 Device Configuration

The device is fabricated by previous group members with optimized ohmic source and drain contacts using Ti/Au metal using the CVD grown few layer sample in close environment (Chapter 2.1). After proper device process technologies, such as rapid thermal anneal (RTA) and ion bombardment, we achieved sheet resistivity of the fabricated two terminal metal semiconductor metal (MSM) device as $\rho_s=1.9\times10^5\ \Omega/\square$, and specific contact resistivity as $\rho_c=8.4\times10^{-5}\ \Omega\times cm^2$ [18]. As shown in Figure 5, the device under test of the low frequency noise study has a channel spacing of 6μm, and the channel length is 50μm. Therefore, we would be able to focus on the device transport mechanisms of the few layer MoS_2 channel itself not associated with interfacial states or traps within the gate dielectric.

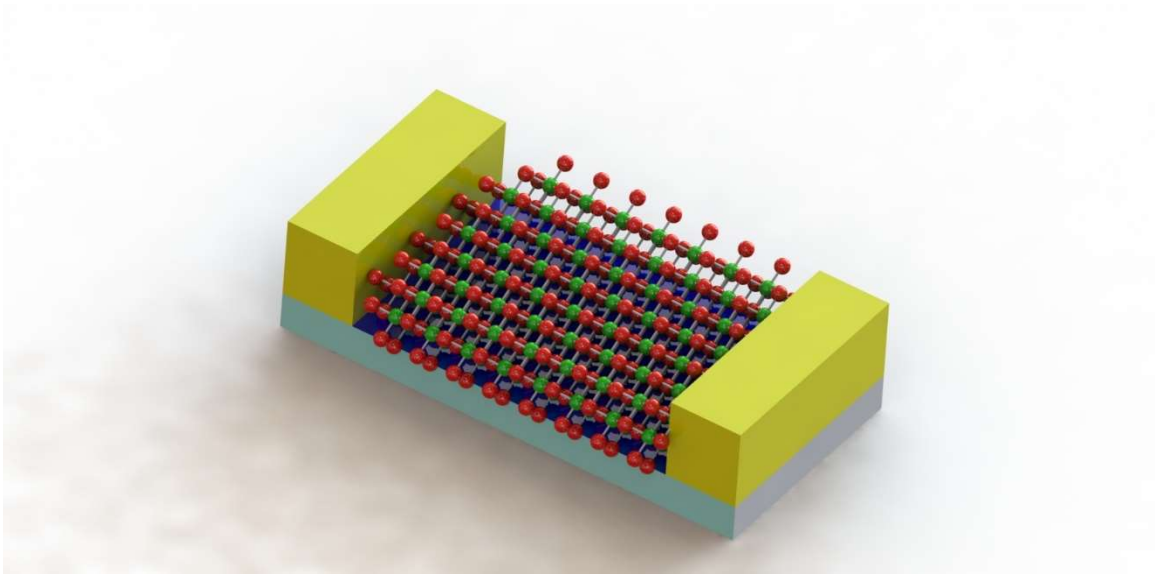

Figure 5: Two-terminal Few Layer MoS_2 Device Under Test.

Chapter 3: Device Carrier Transport Study as Motivation of this study

Previously, researchers have demonstrated temperature dependent carrier transport studies on various mono-layer and few-layer MoS_2 devices [19, 20, 21]. The main conclusion is that the device is dominated by thermally activated band transport at high temperatures, variable range hopping at low temperatures, and resonant tunneling at extremely low temperature [20, 21]. However, the exact temperature regions remain to be idiosyncratic to the material crystal quality, layer thickness, etc. In our previous study (as shown in Figure 6 below) on the specific device under test of this project, it has been proved [21] that the device is dominated by thermally activated band transport when T>180K, Efros-Schklovskii variable range hopping when 50K<T<180K, and resonant tunneling when T<50K.

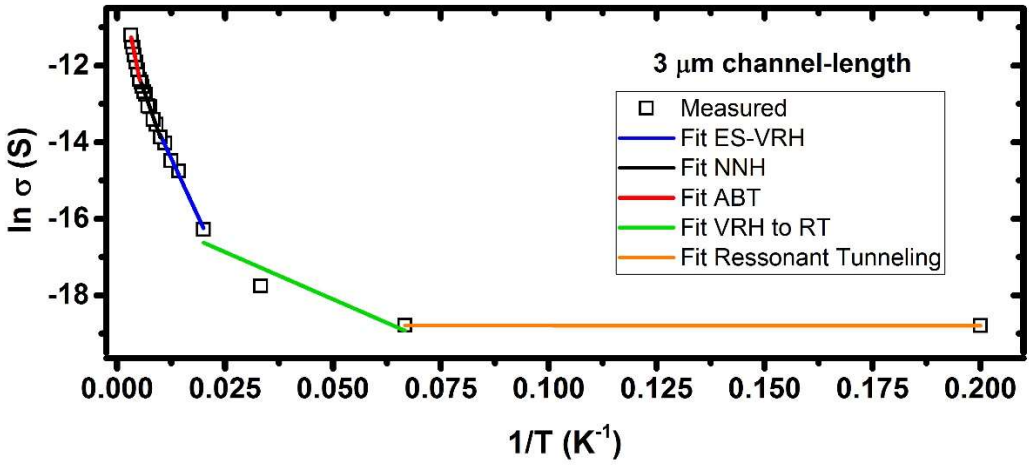

Figure 6: Summary of Device Transport Results.

Such carrier transport mechanisms were studied through the study of AC impedance analysis from 20Hz to 1 MHz with 1V DC bias and 10 mV AC signal amplitude, and DC I-V characteristics from -20V to 20V. Also, by fitting the data to separate regions of I-V curve (Fig. 7a), the mobility and carrier concentration of the device at each temperature could be extracted regarding Mott Gurney law for space charge limited conduction (SCLC) [12] carrier transport in semiconductors (Equation 7). Here L = 50μm is the channel length; t = 6nm is the layer thickness; and d = 6μm is the channel spacing.

$$I = \frac{q\, n\, \mu\, t\, L}{d} V + \frac{2\, \epsilon\, \mu\, L}{\pi\, d^2} V^2 \qquad (4)$$

As shown in the figure 7b, the mobility increases with increasing temperature, which implies that device carrier transport is strongly dominated by defect scattering mechanism. The study of low frequency noise could provide us further information on such dependence of carrier mobility.

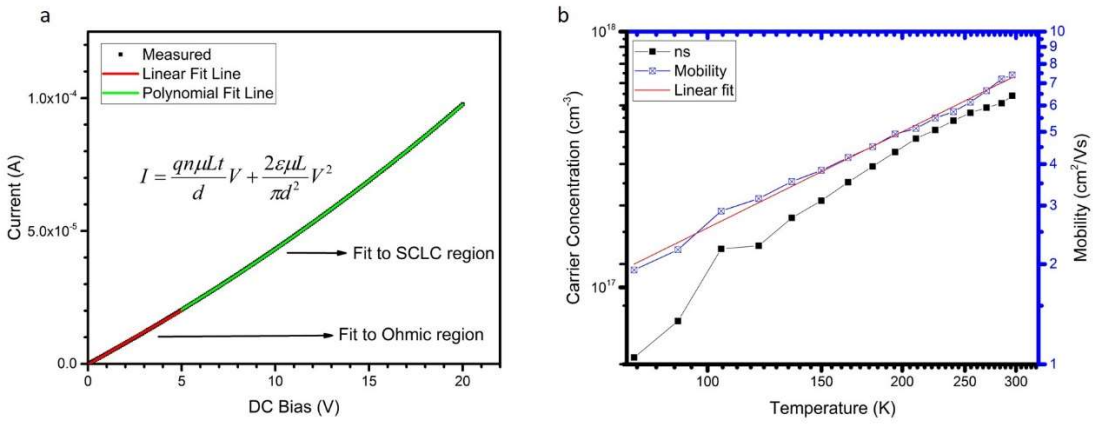

Figure 7: Device DC-IV characteristics under temperature variations (a) Sample I-V characteristics of the device at 300K (b) Extracted mobility and carrier concentration. Mobility was linearly fitted in log-log plot with slope of 0.96±0.02.

Therefore, an important question to answer is that how the low frequency noise in these devices are relevant to the carrier transport mechanisms. This is the motivation of this thesis research: to investigate the correlation between the low frequency noise performance and the carrier transport processes.

Chapter 4: Low Frequency Noise Device Testing Method Design

To properly measure the low frequency noise characteristics of the system, precise controls of input and output signals are required so that the noise spectrum density is accurately measured in the spectrum analyzer. All our measurements were taken place under vacuum condition (10^{-8} Torr) in Lake Shore TTP4 Cryogenic Probe Station. Also, precise measurement of noise was performed using Agilent E4440A Spectrum Analyzer and SR570 Low-Noise Current Preamplifier.

The SR570 provided proper current offset and amplification to the signals before being analyzed by E4440A spectrum analyzer with reducing influence from atmosphere condition. Also, the DC bias of the device was achieved through the battery of SR570 to eliminated systematic power line noise. The detailed setup of the device under test (DUT) is shown in Figure 8 below. The front-end amplifier is applied with feedback resistor to adjust the amplification of input current signal as noise signal sensitivity control and to introduce current offset , filter 1 and 2 is applied as a bandpass filter to focus on the measurement of signal within desired frequency range.

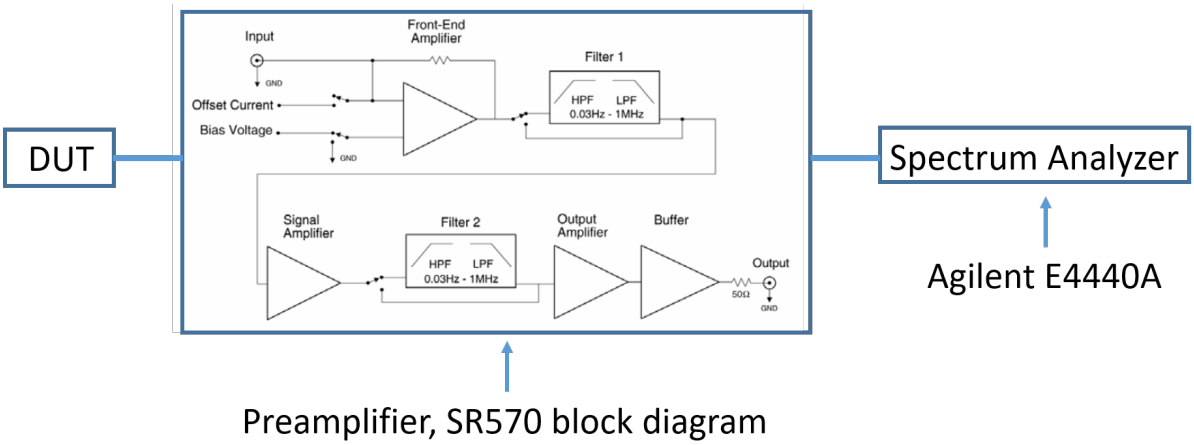

Figure 8: Setup Illustration of Low Frequency Noise Measurement, the block diagram of SR 570 is accessed from [22].

To be able to accurately measure the low frequency noise of the device, the preamplifier was set to sensitivity level of 100 nA/V offer the optimal amplification to the signals over a wide range of temperature. The input current level offset is selected to be as close to the actual current value as possible. The built-in filter of the preamplifier was set to band pass mode ranging from 0.3 Hz to 1 MHz with low noise gain mode. After the output signal from the preamplifier is delivered to the spectrum analyzer. The noise power spectrum density would be measured over the frequency range from 1 Hz to 2 kHz considering the accuracy of preamplifier output. Also, the signal was being measured for 20 times to provide stable and average values of the low frequency noise. Also, to provide the temperature dependent study of the device transport mechanisms, liquid Nitrogen and liquid Helium were used as cryogenic sources for cooling the probe station after the inner chamber was evacuated to 10^{-8} Torr. All of our measurements were thus done in vacuum environment.

Chapter 5: Results and Discussion

The noise on MoS_2 devices are reported to be dependent on layer thickness, contact quality, gate voltage etc [23, 24, 25, 26]. For examples, the normalized noise power spectrum density (PSD_Norm) was determined by channel and contact resistance [26]; "M" shape pattern dependence of PSD_Norm on gate voltage were discovered to be related to trap states [27]; the PSD_Norm increased to maximum magnitude level when there is six layers of MoS2 proposedby the study done by Sharma [23].

Low frequency 1/f noise (LFN) measurements on our few layer device were performed from 10 Hz to 2000 Hz, with 0.5V to 5V applied DC bias. The PSD_Norm (normalized power spectrum density) as shown in Figure 9, and Figure 10 under 55K to 300K indicates the universal validness of f^{β} noise with β close to -1. Also, the β factor in Equation 3 is also extracted as shown in Figure 11 below.

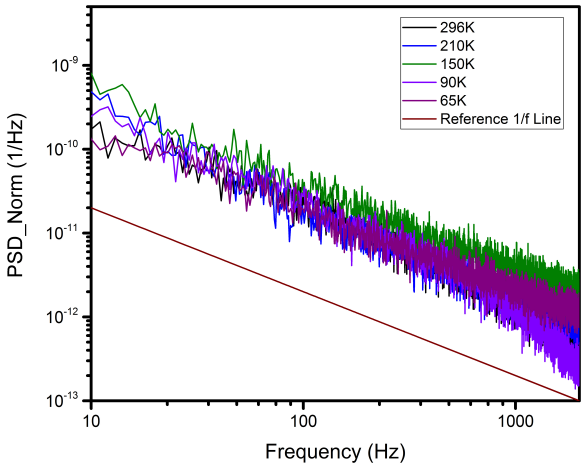

Figure 9: Measured 1/f Noise Spectrum with Temperature Variation at 3V

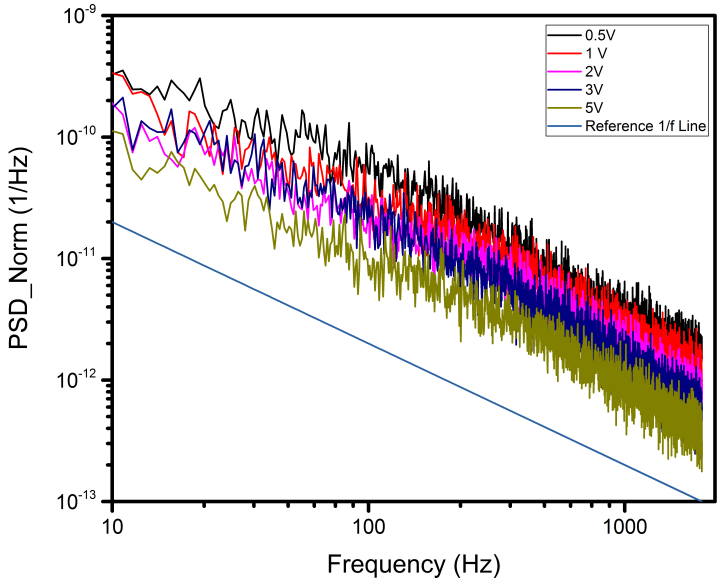

Figure 10: Measured 1/f Noise Spectrum with Biasing Voltage Variation at 300K

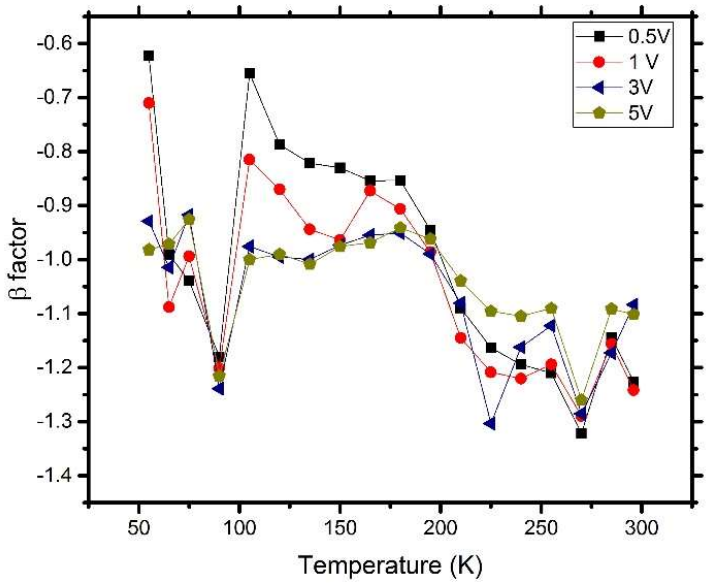

Figure 11: Extraction of β factor in $1/f^{\beta}$ noise over the temperature range under selected biasing voltage condition.

5.1 Low Frequency Noise Performance when T>180K correlated with band transport

The first property to investigate about the noise mechanism is to determine whether it is mobility fluctuation mechanism or carrier number fluctuation mechanism dominant [17]. For mobility fluctuation, one would expect universal validness of Hooge noise model in Equation 5 to Equation 8 [17]. It is shown that the normalized power spectrum density would be following power law dependence of drain current with -1 regardless of the regions of operation. Here W is the channel width, μ is the effective mobility over the entire channel, and L is channel length. Also, the noise could be independent of V_{DS} in subthreshold region as the drain current and total charge Qi is independent when $V_{DS} >>$ kT/q.

$$I_D = W \mu Q_i(x) \, {}^{dV}/_{dx} \qquad \text{in saturation region} \tag{5}$$

$$\frac{S_I}{I^2} = \frac{q \alpha_H}{fWL^2} \int_0^L \frac{dx}{Q_i(x)} = \frac{q \alpha_H}{fWL^2} \int_0^{V_{ds}} \frac{W \mu}{I_D} dV = \frac{q V_{ds,sat} \alpha_H \mu}{f L^2 I_D} \tag{6}$$

$$I_D = \frac{W kT\mu}{q} \, {Q_i(x)}/{dx} \qquad \text{in linear and subthreshold region as dominated by diffusion} \tag{7}$$

$$\frac{S_I}{I^2} = \frac{\alpha_H \mu 2kT}{f L^2 I_D} \tag{8}$$

Another fluctuation mechanism, carrier number fluctuation is caused by generation recombination of carrier numbers in the channel. Such mechanism is mainly analyzed by McWhorter [17]. The main conclusion is that the normalized noise could be modeled

approximately as below in Equation 9. Here λ is the tunneling attenuation length predicted by WKB theory as shown in Equation 10.

$$\frac{S_I}{I^2} = \frac{q^2 kT\lambda N_t}{f\ W\ L\ C_{OX}^2}\ \frac{1}{(V_{GS}-V_T)^2} \tag{9}$$

$$\lambda = (\frac{4\pi}{h}\sqrt{2\ m\ \phi_B})^{-1} \tag{10}$$

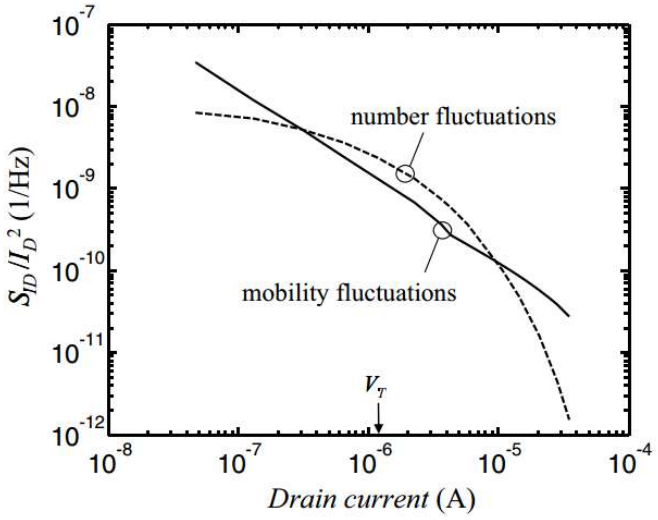

Figure 12: Simulation of noise fluctuation mechanisms on a standard Si p-MOSFET. [17]

Thus, simulation of these two models could be achieved for a regular pMOSFET done by Haartman and Ostling [17] using Equations 6 to 10 as shown in Figure 12 above. And in our study, similar analysis was done under various temperature conditions to reveal the power law dependence of normalized power spectrum density (PSD_Norm) on drain current I_d. Clear trend of linear dependence on the log-log plot of PSD_Norm vs I_d is observed as shown in Figure 13a below, and the linear fit slope is plotted over temperature regime with error bars in Figure 13b. The large errors in some temperatures are attributed

to non-linearity of the trend when the device were biased at higher voltages. As a result, fit slope is around -1 when T>180K.

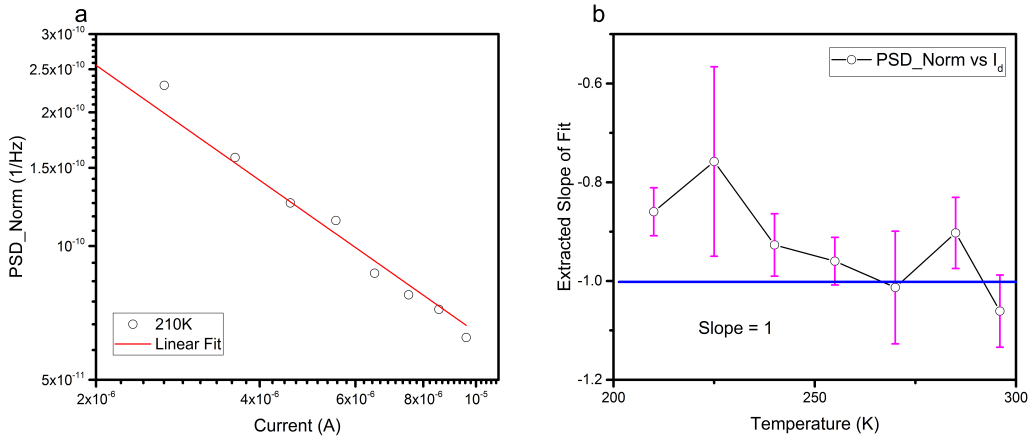

Figure 13: (a) Sample PSD_Norm vs I_d relationship at 210K (b) Temperature dependent analysis of PSD_Norm vs I_d linear fit slope (extracted from Fig. 13a) with error bars

Trend of fit slope closing to -1 gives us evidence that the noise mechanism follows Hooge's mobility fluctuation model when T>180K. Also, the mobility fluctuation dominated device transport is compliable with our expectation regarding the imperfect material quality in each separate layer of the few layer structure. As discussed in the carrier fluctuation model, the change of carrier concentration is derived because of carrier tunneling from the channel to gate terminal through trap states in the insulating layer. The carrier number fluctuation in this device is suppressed since there is no gate terminal introducing change of carrier concentration. Such mobility fluctuation could be caused by mainly impurity scattering mechanisms. Other scattering mechanisms such as surface roughness, and Coulomb scattering caused by floating gate [25] would also be considered in contribution to the mobility fluctuation. Also, this mobility fluctuation mechanism model is derived under the

assumption of carrier injection from source to drain of band transport theory. Therefore, this validated the previous noise transport phenomena study.

Another interesting feature of the spectrum is the peaks values of PSD_Norm over temperature. This forms an "M" shape dependence (Figure 14) of the noise under the previous discussed band transport regime with consistence over all frequencies. Critical transition temperatures around 240K and 270K were discovered.

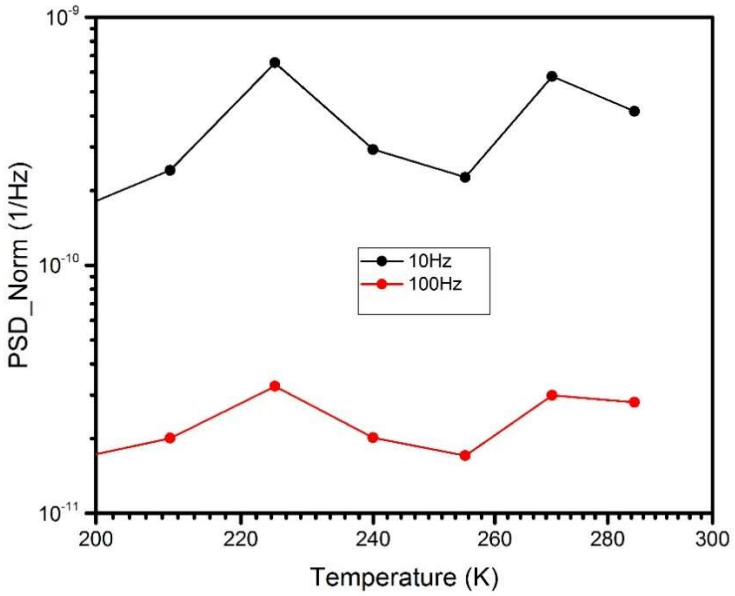

Figure 14: Temperature Dependent Analysis of Normalized Power Spectrum Density at 10Hz and 100Hz.

Similar trends were also observed in graphene and MoS_2 with the variation of gate voltage [27, 28, 29]. In these reports, the origin of this shape comes from the topological structure of the 2D material. The noise power spectrum density follows a V-shape dependence of

gate voltage reaching its minimum level near Dirac point voltage attributed to the spatial charge inhomogeneity [28]. Here in our study, we expect the origin of "W" to be the change of scattering state occupation with temperature variations. When temperature is increased, the scattering relaxation time at certain biasing condition is varied. At 255K, we observe a sudden decrease of noise level, with two other peak spectrum density at 225K and 270K. This is because of the material crystal quality creating various defect states. At these characteristic temperatures, certain defect scattering states population are charged thus changing the effectiveness of mobility fluctuation in carrier transport. As shown in Figure 15, when temperature is further increased (fermi level moves towards conduction band edge), one type of defect scattering state occupation becomes deactivated while another come into dominance as possible S2- vacancies transferred into S1- vacancies with increasing electron population.

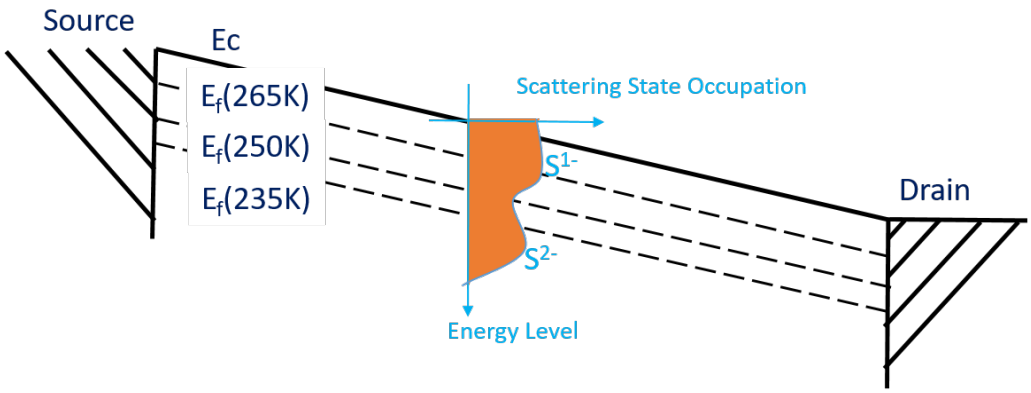

Figure 15: Illustration of proposing mechanism forming "W" shape dependence of normalized power spectrum density over temperature.

Also, the effect of surface roughness scattering mechanisms remains to be another potential cause of such phenomenon. At lower temperature, although there might be potentially other

scattering mechanisms involved to change the spectrum density expected by this model, the noise mechanism itself would not be dominated by such mechanism rather by electron hopping phenomenon (T<180K), which will be discussed later. Therefore, such phenomenon only occurs at this temperature range.

Noise performance influenced by multiple scattering events was also observed in graphene devices [30] originating from elemental scattering event of the device. In abstract, it was described by the elemental mobility fluctuation model by Equation 11 [30], where N_t^{μ} is the concentration of scattering centers contributing to the noise, Λ is the mean free path of the charge carriers, ς is the probability for a scattering center to be in the state with state 1 with cross section σ, V is the channel volume, and τ is the characteristic relaxation time of each defect level.

$$\frac{S_I}{I^2} \propto \frac{N_t^{\mu}}{V} \frac{\tau\, \varsigma\, (1-\varsigma)}{1+(\omega\tau)^2}\, \Lambda^2(\sigma_2 - \sigma_1)^2 \qquad (11)$$

By integrating Equation 11 with appropriate distribution function of relaxation time [30], one would expect the noise to be dominated by 1/f trend. Therefore, when the scattering relaxation time was varied with temperature, noise amplitude would also be varied. Further analysis on such phenomena is to be clarified with study of three terminal devices. Such mechanism must be the dominant effect since the device transport was proved to be mobility fluctuation above.

5.2 Low Frequency Noise Performance when T<180K correlated with variable range hopping transport

Various hopping noise theories were proposed in this area before regarding the cause of fluctuation. Shklovskii [31] proposed the "concentration" model due to fluctuations of the number of electrons belonging to the infinite cluster of donors responsible for conductivity. The fluctuations are caused by slow exchange of electrons between the infinite cluster and isolated donor clusters in the noise with temperature dependent relation in Hooge's parameter. Also, Kozub proposed the "mobility" approach (dipolar model) [32] due to the fluctuation of hopping site energy. The fluctuations are related to changes of local potentials [32] due to electron hopping within some pairs of sites not incorporated into the percolation cluster; such pairs were defined as hopping fluctuators as shown in Figure 16.

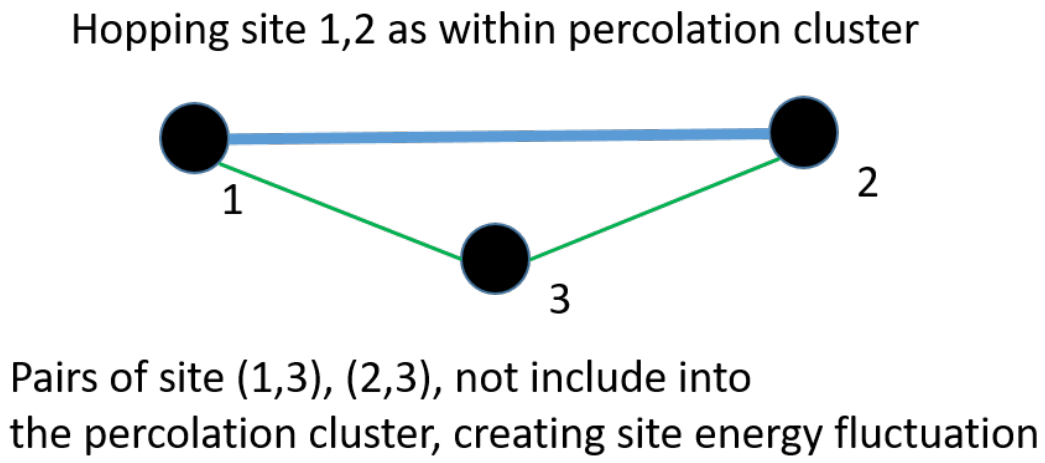

Figure 16: Illustration of Electron Hopping Noise Proposed by Kozub.

Equation 12a was the original theory derived by Kozub based on the exponential hopping conductivity equations as an analog to Hooge's noise relationship, and Equation 12c simplified the terms with the assumption made in Equation 12b, and uniform distribution of fluctuator density of states. Here ($r\varsigma_c/L$) is the percolation cluster behavior factor, P(T) is the dislocation distribution function, l(ω) is the spatial separation between hopping sites forming the fluctuator. Therefore, PSD_Norm would follow the $T^{-3/2}$ dependence for Variable Range Hopping (VRH) [32]. In this case, we assumed $r < R_{min} < l$, where R_{min} is the distant from the hopping sites to a nearest fluctuator. This is based on the comparison of Coulumb center potential and electron hopping range. For variable range hopping, one would have $e^2/l < kT < e^2/r$.

$$\frac{(\delta R)^2_\omega}{R^2} \sim \left(\frac{r\varsigma_c}{L}\right)^3 \frac{P(T)\,T}{\omega}\left[\frac{e^2}{kT}\, r\, l(\omega)\right] \tag{12a}$$

$V \approx \frac{d}{4\pi\varepsilon}\frac{e^2}{r^2}$ for dipolar model of electric potential with dipole spacing as d,

$$\frac{1}{4\pi\varepsilon}\frac{e^2}{r^2} \sim kT,\ r \sim T^{-1/2} \tag{12b}$$

$$\frac{S_I}{I^2} = \frac{(\delta R)^2_\omega}{R^2} \sim T^{-3/2}\ ,\ P(T) = constant \tag{12c}$$

In regards to such mechanisms in our devices, the normalized power spectrum density (PSD_Norm) on a log-log scale as (Fig. 17) showed that PSD_Norm $\propto T^{-k}$ dependence from 75K to 180K with k is close to 3/2, which indicates that the device is dominated by variable range hopping transport mechanism. The results of fitting to the power law slope at 10 Hz is -1.45 ± 0.31, and at 100 Hz is -1.26 ± 0.47 showing the consistence of

hopping noise trend. This overall trend of regional fit corresponds to the dipolar model of Kozub [32] (Equation 12b). The error of our fitting is larger than expected system random error, which involves further investigation of the noise level. Thus, another fitting is performed on the data from 105K to 180K, we achieved a higher value of k around 1.62 ± 0.14 for 10Hz, and 100Hz with the error reduced to a smaller range. Although these two regimes of fitting introduced potential deviation of model from 75K to 105K, variable range hopping noise mechanism from 75K to 180K is still the dominant effect. However, the noise amplitude does not follow the above theory from 55K to 75K. One possible explanation of this irregular trend is the transition of hopping conduction to another transport mechanism when T<50K. The low temperature transport phenomena suggested by previous works is dominated by resonant tunneling [20,21]. From our work, it suggests that the noise transport mechanism would be altered when T<75K.

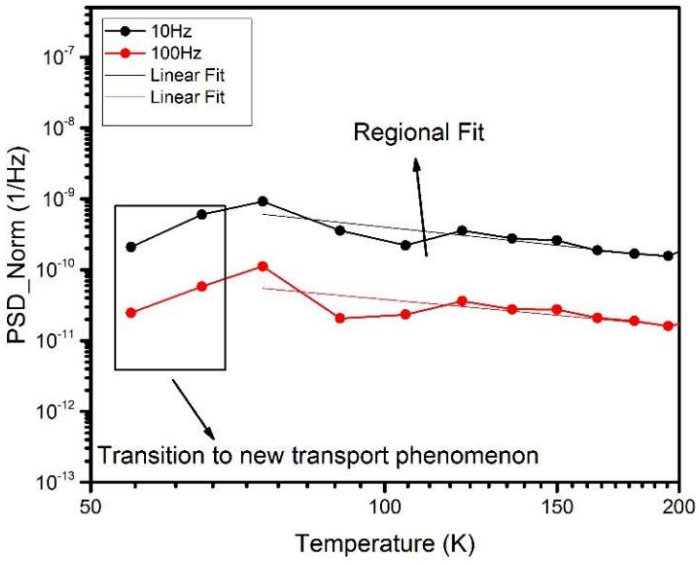

Figure 17: Temperature dependent analysis of normalized noise spectrum density (PSD_Norm) at 3V on log-log scale.

5.3 Low Frequency Noise Performance when T>180K potentially correlated with resonant tunneling transport

When the temperature was lower than 50K, we observed a unique low frequency noise spectrum (Figure 16), which has not been shown before. As reference to previous transport evidence [21], this extremely low temperature regime was dominated by resonant tunneling. The regular Hooge's empirical equation and generation-recombination description of the noise was not valid here to fit the spectrum. Our result implies the resonant of noise spectra under the measured frequency range. There were no studies proven the existence of peaks in the low frequency noise spectrum.

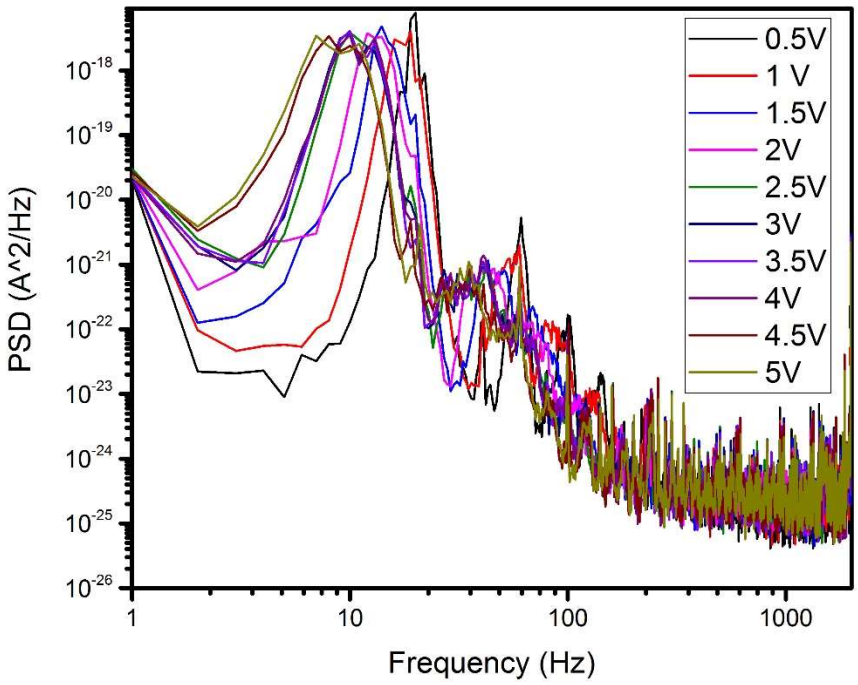

Figure 18: Measured Noise Spectrum at 10K, similar spectra were also observed at other temperature when T<50K

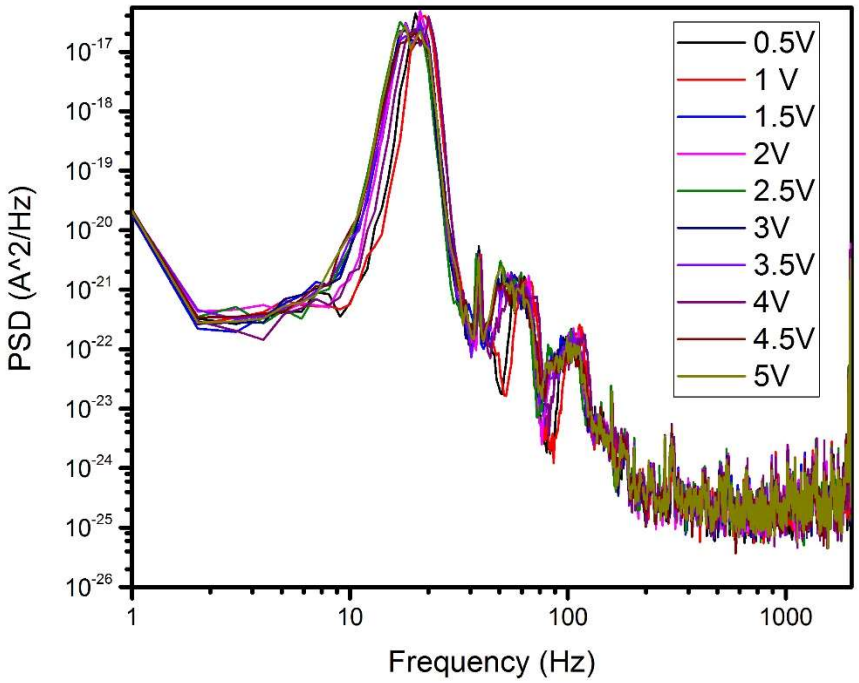

Figure 19: Measured Noise Spectrum at 40K, whereas the frequency dependence of the peak is less obvious than that of 10K

Here we suggest a qualitative explanation of this noise spectrum relating to resonant tunneling. Previously, there have been reports [33] on the resonant tunneling transport phenomena in other systems such as Si Inversion Layers in metal-oxide-semiconductor field-effect transistors. In these devices, non-pure Lorentzian peaks of conductance with variation of gate voltage at extremely low temperatures were observed. This comes from the localization length L_0 in comparison with sample dimension, maximum conductance when the resonant site is at the center of the sample spatially [33]. In our experiment, we applied DC bias on the channel allowing certain occupation of states.

In one biasing condition, the frequency response of the conductance at different frequencies were varied with different biasing condition as the localization length L0 changes, different resonant tunneling sites were activated in response to the frequency signal input. Maximum channel conductance is obtained when resonant site is exactly at the center of the sample. This gives the tiny variation of the conductance which were amplified in the noise spectrum. The shift of the peaks as shown in Figure 18 under different biasing conditions would thus be understood regarding the change of energy to the system. Also, such phenomenon is more obvious at lower temperatures when comparing Figure 18 and Figure 19. To understand this phenomenon, we suggest that there is less occupation of resonant tunneling sites at lower temperatures. Therefore, higher temperature noise spectrum is independent of the DC biasing condition because of the higher carrier occupation of states with increasing thermal energy.

Chapter 6: Conclusion

In this study, we reported the design progress of our study on large area few layer MoS_2 through chemical vapor deposition (CVD) on (0001) oriented sapphire substrate in open environment condition. Limited material coverage of MoS_2 film grown on the substrate was found, which gave us insights on future works in improving this design process. Such process would facilitate the material deposition process design in a wide range of applications.

Also, temperature dependent low frequency noise studies were conducted on our two terminal CVD grown few layer MoS_2 device grown in close environment. Such studies are especially important for devices based on low dimensional semiconductors because of their high surface to volume ratio. The noise spectra and the discussion above gave evidences of transport phenomenon under different temperature regimes corresponding to previous investigations on carrier transport phenomena of such devices [21]. Mobility fluctuation noise mechanism is dominant when T>180K under band transport regime. This was proved by investigating the linear fit slope of normalized noise power spectrum density (PSD_Norm) with DC biasing current. The ubiquitous phenomena of "M" shape temperature dependent (210K<T<265K) on the noise spectrum density was observed. Further theoretical and experimental studies on three terminals gated few layer MoS_2 devices are required for such phenomena. Also, variable range hopping transport was confirmed under 75K<T<180K with the fitting of PSD_Norm to temperature having $T^{-3/2}$ dependence. The deviation from hopping noise trend of noise spectrum density at low

temperatures (50<T<75K) indicated involvement of other noise and transport mechanisms at lower temperatures. These above results gave us the ideas of using low frequency noise study as an effective way to analyze electron transport mechanisms under various conditions. Non-Lorentzian noise spectra were observed when T<50K potentially related to resonant tunneling transport mechanisms. Qualitative explanation of such phenomenon was proposed while requiring further theoretical studies.

References

[1] B. Radisavljevic, A. Radenovic, J. Brivio, V. Giacometti, and A. Kis, "Single-layer MoS2 transistors," Nature Nanotechnology, vol. 6, no. 3, pp. 147–150, 2011.

[2] N. Izyumskaya, D. O. Demchenko, V. Avrutin, Ü. Özgür, and H. Morkoç, "Two-dimensional MoS2 as a new material for electronic devices," Turkish Journal Of Physics, vol. 38, pp. 478–496, 2014.

[3] B. Radisavljevic, M. B. Whitwick, and A. Kis, "Integrated Circuits and Logic Operations Based on Single-Layer MoS2," ACS Nano, vol. 5, no. 12, pp. 9934–9938,

[4] A. K. Geim and I. V. Grigorieva, "Van der Waals heterostructures," Nature, vol. 499, no. 7459, pp. 419–425, 2013.

[5] Q. H. Wang, K. Kalantar-Zadeh, A. Kis, J. N. Coleman, and M. S. Strano, "Electronics and optoelectronics of two-dimensional transition metal dichalcogenides," Nature Nanotechnology, vol. 7, no. 11, pp. 699–712, Jun. 2012.

[6] A. Splendiani, L. Sun, Y. Zhang, T. Li, J. Kim, C.-Y. Chim, G. Galli, and F. Wang, "Emerging Photoluminescence in Monolayer MoS2," Nano Letters, vol. 10, no. 4, pp. 1271–1275, 2010.

[7] K. S. Novoselov, "Electric Field Effect in Atomically Thin Carbon Films," Science, vol. 306, no. 5696, pp. 666–669, 2004.

[8] M. S. Fuhrer and J. Hone, "Measurement of mobility in dual-gated MoS2 transistors," Nature Nanotechnology, vol. 8, no. 3, pp. 146–147, May 2013.

[9] M.-H. Doan, Y. Jin, S. Adhikari, S. Lee, J. Zhao, S. C. Lim, and Y. H. Lee, “Charge Transport in MoS2/WSe2 van der Waals Heterostructure with Tunable Inversion Layer,” ACS Nano, 2017.

[10] D. Pierucci, H. Henck, J. Avila, A. Balan, C. H. Naylor, G. Patriarche, Y. J. Dappe, M. G. Silly, F. Sirotti, A. T. C. Johnson, M. C. Asensio, and A. Ouerghi, “Band Alignment and Minigaps in Monolayer MoS2-Graphene van der Waals Heterostructures,” Nano Letters, vol. 16, no. 7, pp. 4054–4061, 2016.

[11] G. C. A. Z. Magda, J. Pető, G. Dobrik, C. Hwang, L. P. Biró, and L. Tapasztó, “Exfoliation of large-area transition metal chalcogenide single layers,” Scientific Reports, vol. 5, p. 14714, Jul. 2015.

[12] M. R. Laskar, L. Ma, S. Kannappan, P. S. Park, S. Krishnamoorthy, D. N. Nath, W. Lu, Y. Wu, and S. Rajan, “Large area single crystal (0001) oriented MoS2,” Appl. Phys. Lett. Applied Physics Letters, vol. 102, no. 25, p. 252108, 2013.

[13] G. Siegel, Y. P. V. Subbaiah, M. C. Prestgard, and A. Tiwari, “Growth of centimeter-scale atomically thin MoS2 films by pulsed laser deposition,” APL Materials, vol. 3, no. 5, p. 056103, 2015.

[14] T. Ohashi, K. Suda, S. Ishihara, N. Sawamoto, S. Yamaguchi, K. Matsuura, K. Kakushima, N. Sugii, A. Nishiyama, Y. Kataoka, K. Natori, K. Tsutsui, H. Iwai, A. Ogura, and H. Wakabayashi, “Multi-layered MoS2 film formed by high-temperature sputtering for enhancement-mode nMOSFETs,” Japanese Journal of Applied Physics, vol. 54, no. 4S, 2015.

[15] A. V. der Ziel, Noise in solid state devices and circuits. New York: Wiley, 1986.

[16] P. Handel, “Fundamental quantum 1/f noise in semiconductor devices,” IEEE Transactions on Electron Devices, vol. 41, no. 11, pp. 2023–2033, 1994.

[17] M. von. Haartman and Östling Mikael, Low-Frequency Noise In Advanced Mos Devices. Dordrecht: Springer, 2007.

[18] X. Luo, “Few-Layer MoS2 Thin Films Grown by Chemical Vapor Deposition,” Thesis. Electrical Engineering, The Ohio State University, 2014.

[19] H. Qiu, T. Xu, Z. Wang, W. Ren, H. Nan, Z. Ni, Q. Chen, S. Yuan, F. Miao, F. Song, G. Long, Y. Shi, L. Sun, J. Wang, and X. Wang, “Hopping transport through defect-induced localized states in molybdenum disulphide,” Nature Communications, vol. 4, 2013.

[20] S. Ghatak, A. N. Pal, and A. Ghosh, “Nature of Electronic States in Atomically Thin MoS2Field-Effect Transistors,” ACS Nano, vol. 5, no. 10, pp. 7707–7712, 2011.

[21] S. Poehler, “Transport Phenomena of CVD Few-Layer MoS2 As-grown on an Al2O3 Substrate,” Thesis. Electrical Engineering, The Ohio State University, 2015.

[22] “MODEL SR570 Low-Noise Current Preamplifier,” Stanford Research Systems. [Online]. Available: http://www.thinksrs.com/downloads/PDFs/Manuals/SR570m.pdf [Accessed: 12-Apr-2017].

[23] D. Sharma, A. Motayed, P. B. Shah, M. Amani, M. Georgieva, A. G. Birdwell, M. Dubey, Q. Li, and A. V. Davydov, “Transfer characteristics and low-frequency noise in single- and multi-layer MoS2 field-effect transistors,” Applied Physics Letters, vol. 107, no. 16, p. 162102, 2015.

[24] D. Sharma, M. Amani, A. Motayed, P. B. Shah, A. G. Birdwell, S. Najmaei, P. M. Ajayan, J. Lou, M. Dubey, Q. Li, and A. V. Davydov, "Electrical transport and low-frequency noise in chemical vapor deposited single-layer MoS2 devices," Nanotechnology, vol. 25, no. 15, p. 155702, 2014.

[25] V. K. Sangwan, H. N. Arnold, D. Jariwala, T. J. Marks, L. J. Lauhon, and M. C. Hersam, "Low-Frequency Electronic Noise in Single-Layer MoS2 Transistors," Nano Letters, vol. 13, no. 9, pp. 4351–4355, Nov. 2013.

[26] M.-K. Joo, B. H. Moon, H. Ji, G. H. Han, H. Kim, G. Lee, S. C. Lim, D. Suh, and Y. H. Lee, "Understanding Coulomb Scattering Mechanism in Monolayer MoS2 Channel in the Presence of h-BN Buffer Layer," ACS Applied Materials & Interfaces, vol. 9, no. 5, pp. 5006–5013, 2017

[27] X. Xie, D. Sarkar, W. Liu, J. Kang, O. Marinov, M. J. Deen, and K. Banerjee, "Low-Frequency Noise in Bilayer MoS2 Transistor," ACS Nano, vol. 8, no. 6, pp. 5633–5640, 2014.

[28] A. A. Balandin, "Low-frequency 1/f noise in graphene devices," Nature Nanotechnology, vol. 8, no. 8, pp. 549–555, May 2013.

[29] G. Xu, C. M. Torres, Y. Zhang, F. Liu, E. B. Song, M. Wang, Y. Zhou, C. Zeng, and K. L. Wang, "Effect of Spatial Charge Inhomogeneity on 1/fNoise Behavior in Graphene," Nano Letters, vol. 10, no. 9, pp. 3312–3317, Aug. 2010.

[30] A. P. Dmitriev, M. E. Levinshtein, and S. L. Rumyantsev, "On the Hooge relation in semiconductors and metals," Journal of Applied Physics, vol. 106, no. 2, p. 024514, 2009.

[31] B. Shklovskii, “Theory of noise for hopping conduction,” Solid State Communications, vol. 33, no. 3, pp. 273–276, 1980.

[32] V. Kozub, “Low-frequency noise due to site energy fluctuations in hopping conductivity,” Solid State Communications, vol. 97, no. 10, pp. 843–846, 1996.

[33] A. B. Fowler, G. L. Timp, J. J. Wainer, and R. A. Webb, “Observation of resonant tunneling in silicon inversion layers,” Physical Review Letters, vol. 57, no. 1, pp. 138–141, Jul. 1986.